CONJUGATE CONVECTION WITH SURFACE RADIATION FROM AN OPEN CAVITY WITH MULTIPLE NON-IDENTICAL DISCRETE HEAT SOURCES

A PROJECT REPORT

SUBMITTED BY

Mr. V. RAVI SANKAR

UNDER THE ESTEEMED GUIDANCE OF

Dr. C. GURURAJA RAO

PROFESSOR

DEPARTMENT OF MECHANICAL ENGINEERING

NATIONAL INSTITUTE OF TECHNOLOGY

WARANGAL-506004, A.P., INDIA

ABSTRACT

All the important results of parametric studies performed on conjugate convection with surface radiation from a rectangular open cavity equipped with four non-identical flush-mounted discrete heat sources are presented here. The governing equations for temperature distribution are evolved through appropriate energy balance between heat generated, conducted, convected and radiated from the cavity. Air, a radiatively transparent medium, is considered to be the cooling agent. The governing equations are later discretized into algebraic form using finite difference formulation and are subsequently solved simultaneously using Gauss-Seidel iterative solver. Full relaxation on temperature has been used along with stringent convergence criterion 10^{-8}. A computer code is written for the purpose. A number of parametric studies showcasing the effects of the independent parameters, like aspect ratio, surface emissivity, thermal conductivity and convection heat transfer coefficient, on various important results are made. Efforts are made to highlight the role played by radiation in the present problem.

KEYWORDS

Conjugate convection, Surface radiation, Open rectangular cavity, Multiple discrete heat sources, Interaction.

LIST OF SYMBOLS

AR	aspect ratio, L/W
F (i, j)	view factor of an element i with reference to another element j of the enclosure
h	convection heat transfer coefficient, W/m^2 K
i	grid numbers along the cavity
j	grid numbers across the cavity
J(i)	radiosity of an element i of the enclosure, W/m^2
k	thermal conductivity of the walls of the cavity including heat source portions, W/m K

L	height of the cavity, m
L_{h1}, L_{h2}, L_{h3}, L_{h4}	heights of discrete heat sources 1, 2, 3 and 4, respectively, m
M_1	grid number at the top end of the first heat source
M_2	grid number at the bottom end of the second heat source
M_3	grid number at the top end of the second heat source
M_4	grid number at the bottom end of the third heat source
M	total number of nodes along the left and right walls of the cavity
N	total number of nodes along the bottom wall of the cavity
n	total number of elements in the enclosure
q_v	volumetric heat generation in each heat source, W/m^3
t	thickness of each wall of the cavity, m
T_{max}	maximum temperature of the cavity, ^oC
$T(i)$	local temperature of a given element i of the cavity, ^oC
T_∞	characteristic temperature of air, ^oC
W	width of the cavity, m
x	co-ordinate direction along the cavity
y	co-ordinate direction across the cavity

Greek symbols

δ_c	convergence criterion in percentage, $\left\lvert\frac{T_{new}-T_{old}}{T_{new}}\right\rvert \times 100$
Δx_{hs}	height of wall element in the heat source portions along the cavity, m

Δx_{nhs}	height of wall element in the non-heat source portions along the cavity, m
Δy	width of wall element across the cavity, m
ε	surface emissivity of walls of the cavity
σ	Stefan-Boltzmann constant (5.6697×10^{-8} W/m^2 K^4)

Subscripts

cond, x, in	conduction heat transfer into an element along the cavity
cond, x, out	conduction heat transfer out of an element along the cavity
cond, y, in	conduction heat transfer into an element across the cavity
cond, y, out	conduction heat transfer out of an element across the cavity
conv	convection heat transfer from an element
gen	volumetric heat generation in an element
new, old	temperatures from current and previous iterations, respectively

1. INTRODUCTION

Literature provides a number of analytical, numerical and experimental studies addressing free, forced or mixed convection without or with the interaction of conduction and surface radiation. With regard to multi-mode heat transfer studies, the first notable work appears to be the one from Zinnes (1970). He came out with his results of the problem of conjugate laminar natural convection from a finitely thick vertical flat plate that has an arbitrary surface heating distribution over it. Lee and Yovanovich (1989) reported a quasi-analytical model on conjugate heat transfer from a two-dimensional vertical flat plate possessing arbitrarily sized discrete heat sources dissipating heat only through free convection. Kang and Jaluria (1990) investigated, experimentally, free convection heat transfer from a heat source module of finite thickness that is mounted on a vertical or horizontal surface.

Kishinami et al. (1995) made a numerical and experimental study on laminar mixed convection from a vertical composite plate equipped with isolated and discontinuous surface heating elements. They simplified their problem by neglecting conduction of heat along the unheated portions of the plate. The problem of electronic cooling involving steady flow of a viscous fluid past a heated strip on a flat plate has been numerically addressed by Cole (1997) making use of scaling principles. Mendez and Trevino (2000) solved, numerically, conjugate free convection from a thin vertical strip with non-uniform internal heat generation. They obtained the non-dimensional temperature distribution along the strip as a function of distribution and intensity of heat sources, aspect ratio, longitudinal heat conductance and Prandtl number.

A probe into two-dimensional steady incompressible conjugate laminar mixed convection with surface radiation from a vertical plate with a flush-mounted discrete heat source has been attempted by Gururaja Rao et al. (2001) using finite volume method. The uniqueness of their work has been that they tackled the governing fluid flow and heat transfer equations without boundary layer approximations. Continuing on the above work, Gururaja Rao (2004) numerically investigated buoyancy-aided conjugate mixed convection with surface radiation from a vertical electronic board having a traversable flush-mounted discrete heat source. He varied the heat source position between the leading and trailing edges of the board covering as many as thirteen positions for the same. Kanna and Das (2005) reported an analytical solution for conjugate forced convection from a flat plate that is exposed to laminar jet flow making use of boundary layer approximations.

Gururaja Rao et al. (2005) reported findings of a numerical probe into conjugate convection with radiation from a square shaped electronic device with multiple embedded discrete heat sources. The geometry of a vertical channel with multiple discrete heat sources in its left wall and involved in multi-mode heat transfer has been tackled numerically by Gururaja Rao (2007). Sawant and Gururaja Rao (2010) solved the problem of combined conduction-mixed convection-surface radiation from a uniformly heated vertical plate. They obtained useful correlations for maximum non-dimensional plate temperature, average non-dimensional plate temperature and mean friction coefficient based on a large set of numerical data generated from their computer code. Very recently Ganesh Kumar and Gururaja Rao (2012) reported simulation

studies and also provided a number of correlations pertaining to the problem of conjugate mixed convection with radiation from a discretely and non-identically heated vertical plate.

A detailed review of literature concerning multi-mode heat transfer, a brief account of which has been provided above, hints that comprehensive parametric studies on a rectangular open cavity containing multiple and non-identical flush-mounted discrete heat sources are not available. Owing to the above, the present paper attempts exhaustive numerical studies on interaction of surface radiation with conjugate convection from an open rectangular cavity possessing four non-identical heat sources flush-mounted in its walls.

2. PROBLEM DEFINITION AND MATHEMATICAL FORMULATION

Figure 1 shows the schematic of the problem geometry considered for the present study. It comprises a vertical rectangular open cavity of height L and width W. An aspect ratio (AR) is defined as L/W. For a given height (L) of the cavity, an increasing AR implies a narrower cavity, while the cavity gets wider with decreasing AR. There are four discrete heat sources flush-mounted in the cavity. As can be seen, the heat sources are non-identical in their height. The left wall of the cavity has three heat sources of heights, respectively, L_{h1}, L_{h2} and L_{h3}, with the longest and the shortest heat sources at the bottom and top ends of the wall. The remaining heat source of the left wall is provided at its centre. Further, the right wall has a solitary heat source of height L_{h4} (= L_{h2}) that is centrally located in it. The bottom wall of the cavity acts as a heat sink helping in the percolation of heat generated in the four heat sources. The walls of the cavity as well as the heat sources are of thickness t (<< L and W). Owing to the above, heat conduction in the walls of the cavity is one dimensional with negligible transverse temperature gradients in them. The walls as well as the heat sources are assumed to be of identical thermal conductivity k, while ε is considered to be their surface emissivity. There is volumetric heat generation at q_v W/m^3 in each of the heat sources. Though q_v and t are identical for all the heat sources, with their heights being different, the net rate of heat generation would be different in different heat sources (however, obviously, the central heat sources in the left and right walls are of identical net rate of heat generation). All the exterior surfaces of the cavity are assumed to be adiabatic implying that heat transfer takes place only from its internal surfaces.

The heat generated in the four heat sources is conducted along the walls of the cavity and is eventually surrendered by combined modes of convection and radiation to air (cooling agent) that is assumed to be radiatively non-participating. The characteristic temperature of the cooling agent is considered as T_∞, while h is considered to be the convection heat transfer coefficient. The figure also shows the coordinate directions chosen for study.

The temperature distribution along the cavity is obtained by establishing energy balance between the heat generated, conducted, convected and radiated. The radiation related terms are tackled by radiosity-irradiation formulation, while for computing the view factors, therein, Hottel's crossed-string method is employed. The cavity here can be divided into different domains namely, heat source portions, interface between heat source and non-heat source portions, non-heat source portions, top adiabatic ends and corners of the cavity.

Invoking energy balance on the element within one of the heat sources, the governing equation is obtained as:

$$q_{gen} + q_{cond,x,in} = q_{cond,x,out} + q_{conv} + q_{rad} \quad (1)$$

After incorporating pertinent expressions for various terms in the above equation and simplifying, it transforms into:

$$kt\frac{\partial^2 T(i)}{\partial x^2} + q_v t - h[\,T(i) - T_\infty] - \frac{\varepsilon}{1-\varepsilon}[\sigma T^4(i) - J(i)] = 0 \quad (2)$$

where J(i) is the radiosity of the given element i that is defined as,

$$J(i) = \varepsilon\sigma T(i)^4 + (1-\varepsilon)\sum_{j=1}^{n} F(i,j)\,J(j) \quad (3)$$

Here, F(i,j) indicates the view factor of the element under consideration with reference to each of the n elements of the enclosure including itself. Equation (1) is extended to the interface between the bottommost heat source and the adjacent non-heat source portion that results in the governing equation for the temperature distribution as:

$$kt\frac{\partial^2 T(M_1)}{\partial x^2} + q_v\left(\frac{\Delta x_{hs} t}{\Delta x_{hs} + \Delta x_{nhs}}\right) - h[\,T(M_1) - T_\infty] - \frac{\varepsilon}{1-\varepsilon}[\sigma T^4(M_1) - J(M_1)] = 0 \quad (4)$$

Similarly, the temperature variation of an interior element present in any of the two non-heat source portions of the left wall would turn out to be in accordance with:

$$kt\frac{\partial^2 T(i)}{\partial x^2} - h[\,T(i) - T_\infty] - \frac{\varepsilon}{1-\varepsilon}[\sigma T^4(i) - J(i)] = 0 \qquad (5)$$

Performing energy balance at the top adiabatic end of the left wall of the cavity, one gets:

$$q_{cond,x,in} + q_{gen} = q_{conv} + q_{rad} \qquad (6)$$

Appropriate substitution of pertinent expressions for different terms in the above equation yields the governing equation for the temperature to be:

$$kt\frac{\partial T(M)}{\partial x} - q_v\left(\frac{\Delta x_{hs} t}{2}\right) + h\left(\frac{\Delta x_{hs}}{2}\right)[\,T(M) - T_\infty] + \frac{\varepsilon}{1-\varepsilon}\left(\frac{\Delta x_{hs}}{2}\right)[\sigma T^4(M) - J(M)] = 0 \qquad (7)$$

The left and the bottom walls would both contribute to the temperature of the left corner of the cavity. Using appropriate energy balance on the element concerned, the governing equation comes out as:

$$kt\left[\frac{\partial T(1)}{\partial x} + \frac{\partial T(1)}{\partial y}\right] + q_v\left(\frac{\Delta x_{hs} t}{2}\right) - h\left(\frac{\Delta x_{hs} + \Delta y}{2}\right)[T(1) - T_\infty] -$$

$$\frac{\varepsilon}{1-\varepsilon}\left(\frac{\Delta x_{hs} + \Delta y}{2}\right)[\sigma T^4(1) - J(1)] = 0 \qquad (8)$$

A similar approach as above is extended further to fetch the governing equations for the temperature distribution of the rest of the computational domain.

3. METHOD OF SOLUTION AND RANGE OF PARAMETERS

The governing equations for temperature distribution in the entire computational domain obtained as above are in the form of partial differential equations. They are converted into algebraic form using finite difference formulation and are later solved simultaneously using Gauss-Seidel iterative method. Full relaxation (relaxation parameter = 1) is used on temperature during iterations. A convergence criterion (δ_c) of 10^{-8} is used to terminate the iterations. The solution is obtained using an explicitly written computer code. The solution obtained comprises

local temperature distribution of the cavity, maximum cavity temperature and contributory roles of convection and radiation in heat dissipation.

As one of the checks for testing the correctness of the code, calculations are made to obtain net rate of heat dissipation from the cavity. To do this, numerical integration has been performed on local convection and radiation heat fluxes along the cavity. The discrepancy between the net rate of heat generated in the cavity and the net rate of heat dissipation from the cavity is calculated over various arbitrarily chosen input parameters. An excellent check for energy balance is noticed with maximum deviation restricted to $\pm$ 0.2%.

All the results pertaining to the present problem are obtained considering certain fixed input parameters. They include L = 20cm, t = 1.5mm, L_{h1} = 6cm, L_{h2} = L_{h4} = 4cm and L_{h3} = 2cm. Further, the characteristic temperature of air (T_∞) is taken to be 25^{o}C. As already defined, the width (W) of the cavity varies in accordance with aspect ratio (AR) chosen. The aspect ratio is varied between 1 and 20 simulating, respectively, broadest and narrowest cavities. Surface emissivity (ε) of the cavity is generally considered to vary between 0.05 (poor emitter or good reflector) and 0.85 (good emitter). However, for a couple of studies involving extraction of exclusive effect of radiation, even ε = 0 (no radiation) and ε = 0.99 (best possible radiation) too are considered. With regard to thermal conductivity (k) of the cavity, a range of $0.25 \leq k \leq 10$ W/m K is used keeping in mind that electronic boards are typically made of materials of thermal conductivity of the order of unity (example : Mylar coated epoxy glass has k = 0.26 W/m K). The convection heat transfer coefficient (h) is varied between 5 W/m^2 K (asymptotic limit for free convection) and 100 W/m^2 K (asymptotic limit for forced convection) thus capturing the entire convection regime.

4. RESULTS AND DISCUSSION

It is appropriate to arrive at the optimum grid system for discretization of the computational domain before initiating parametric studies. In order to do this, a study is performed for a fixed set of input comprising $q_v = 5 \times 10^5$ W/m^3, AR = 1, k = 0.25 W/m K, ε = 0.45 and h = 5 W/m^2 K. Various combinations of M, M_1, M_2, M_3, M_4 and N have been tried changing one at a time. Sensitivity of the grid size is tested with regard to the maximum cavity temperature (T_{max}) and percentage discrepancy between the net rates of heat generation and

dissipation. From the results of the above study, it is observed that T_{max} gives the best possible convergence within $\pm$ 0.003% along with acceptable energy balance check for M = 241, M_1 = 91, M_2 = 106, M_3 = 166, M_4 = 211 and N = 31. In light of this, the ensuring parametric studies are performed using the grid system frozen as above.

4.1 Variation of local temperature distribution along the cavity with other parameters

In order to study the role surface emissivity (ε) plays in influencing the local temperature distribution along the walls of the cavity, results are obtained for a given input [$q_v = 5 \times 10^5$ W/m^3, AR = 1, k = 0.25 W/m K and h = 5 W/m^2 K]. Three typical values of ε are chosen with 0.05 and 0.85, as already indicated, respectively, signifying poor and good emitters, while an average emitter being assigned a value ε = 0.45. Figures 2(a), (b) and (c), respectively, describe the results thus obtained along the left, bottom and right walls of the cavity. It can be seen from Fig. 2(a) that, for a given ε, the temperature variation along the left wall is wavy with three local maxima and two local minima. The reason for the above may be attributed to the discreteness in heat generation in the wall. It is further noticed that the temperature drops from one local maximum to the subsequent local minimum and then rises to the next local maximum in the non-heat source portions of the left wall rather sharply. The maximum left wall temperature is noticed in the bottommost heat source somewhere around its geometric centre. Another feature of the same figure is that the second local minimum is far lower than the first local minimum. This is due to a relatively longer non-heat source portion between the central and the topmost heat sources compared to the one between the bottommost and the central heat sources.

The figure further shows that though the nature of variation of temperature is similar for all the values of ε chosen, a significant drop in local temperature occurs with increasing ε. However, two exceptions are noticed in this context. Firstly, the drop in temperature with increasing ε is quite significant in the heat source portions of the wall. Secondly, in a narrow portion, somewhere at the second non-heat source portion of the left wall, a crossing of temperature profiles in noticed with temperature, in that limited portion, showing a slight increase with increasing emissivity. The first exception is attributed to the fact that there is a major heat transfer activity at the heat source portions of the wall. With regard to the second exception mentioned above, the possible reason could be changes occurring in irradiation and emissive power of the left and right walls of the cavity. In the present example, the first local

peak temperature is observed to be coming down by 39.29% as ε is increased from 0.05 to 0.85. Figure 2(b) indicates that, barring an initial short length from the left bottom corner, the local temperature increases along the bottom wall of the cavity with increasing ε owing to reasons already explained. Figure 2(c) pertaining to the right wall of the cavity shows that there is a marked drop in temperature with increasing ε at and also in the vicinity of the central heat source portion. In the rest of the portion of the right wall, yet again, the temperature rises with increasing ε, just similar to that noticed along the bottom wall. Expectedly, a single local peak is noticed near the geometric centre of the right wall. In the present example, the local right wall temperature at its top adiabatic end is increasing by 38.78% as ε is increased to 0.85 from 0.05.

In order to investigate the nature of variation of the local temperature distribution along the cavity in the entire regime of convection, Figs. 3 (a), (b) and (c) are plotted for the case with $q_v = 5 \times 10^5$ W/m^3, AR = 1, k = 0.25 W/m K and ε = 0.45. Five different values of h (5, 10, 25, 50 and 100 W/m^2 K) are considered, with h = 5 W/m^2 K and h = 100 W/m^2 K indicating asymptotic free and forced convection limits, respectively. The general trend followed by the left, bottom and right wall temperature profiles is similar to what has been noticed in the earlier study (Fig. 2). Further, the figure shows an expected decrement in local temperature with increasing h. However, the above effect of h is quite substantial to begin with, while it gets diminished towards the forced convection dominant regime. In the present example, a marked drop of 52.15% in T(x) at the top adiabatic end of the left wall is noticed between h = 5 W/m^2 K and 25 W/m^2 K, while a comparatively smaller drop of 37.66% is observed as h is increased from 25 W/m^2 K to 100 W/m^2 K. Figure 3(b) shows the temperature profile of the bottom wall in various convection regimes. It indicates a sharp drop in temperature in the initial portion of the wall that gets almost notional towards the end of the wall. Like the left wall, the bottom one too has its temperature greatly influenced by h between 5 and 25 W/m^2 K. A similar trend is observed from Fig. 3(c) that pertains to the right wall of the cavity, whose central temperature diminishes by 53.19% between h = 5 and 25 W/m^2 K and 37.94% between h = 25 and 100 W/m^2 K. The observations from the present study tacitly hint that h = 25 W/m^2 K is an optimum value of convection heat transfer coefficient with no significant benefit resulting from increasing the flow velocity of air for increasing h, holding other parameters fixed.

The effect of thermal conductivity of the material of the cavity on the local temperature distribution is described in Fig. 4. Four values of k (0.25, 0.5, 0.75 and 1 W/m K) are selected for the study, and the rest of the fixed input taken up is also shown. As can be seen, the general trend of the temperature for a given value of k is similar to that observed in Figs. 2 and 3. However, crossing of temperature profiles pertaining to left and right walls is observed as one moves from heat source portion to non-heat source portion of the concerned wall. In other words, as thermal conductivity increases, the local temperature in all the heat source portions decreases, while it increases in the non-heat source portions. Both these phenomena may be attributed to enhanced rate of percolation of heat from the heat source portion owing to increased thermal conductivity k. In the case considered here, the temperature at the centre of the left wall decreases by 9.49% as k increases from 0.25 W/m K to 1 W/m K and a rise of 25.48% is observed at the centre of the adjacent non-heat source portion (second non-heat source portion) as k varies between the above mentioned limits. The same exercise, in comparison, is bringing a drop in temperature at the centre of the heat source portion of the right wall by 10.81%.

4.2 Extraction of explicit effect of radiation on local temperature distribution

In an attempt to separate out the role surface radiation plays in dictating the local temperature profiles along the left and right walls of the cavity, Fig. 5 is drawn for a fixed set of input parameters shown. Two distinct cases have been chosen, viz., $\varepsilon = 0$, signifying non-consideration of radiation, and $\varepsilon = 0.99$, simulating consideration of radiation with the best possible emitting surface. The figure unequivocally underlines the role radiation exhibits both on left and right wall temperature profiles. One can clearly notice a huge drop in local temperature, specifically along heat source portions, when once radiation is reckoned with employing the best possible emitter, say lampblack. For example, with regard to the left wall of the cavity, the peak temperature noticed in the bottommost heat source comes down by a very large 44.42% on employing radiation with $\varepsilon = 0.99$ when compared to ignoring it all together. The current study, thus, cautions against overlooking radiation in any regime of convection, in general, and in free convection dominant regime, in particular.

4.3 Variation of maximum temperature of the cavity with other parameters

The maximum temperature (T_{max}) attained and its control would be the basic objectives of a heat transfer engineer working in electronic cooling applications. On account of the above, a probe into dependence of T_{max} on different pertinent independent parameters is mandatory.

The variation of T_{max} with ε in different regimes of convection is plotted in Fig 6. Four typical values of h are considered for the present study and the other input parameters like q_v, AR and k are held constant and are shown in the figure. A monotonic drop in T_{max} with ε is observed for free convection dominant regime (h = 5 W/m^2 K) on account of increase in radiative dissipation from the cavity with other parameters remaining constant. Though the trend is similar for other values of h too, the degree of decrease of T_{max} with ε gets progressively less pronounced as one moves towards forced convection dominant regime. This may be attributed to the overriding effect of convection here. In the present example, T_{max} drops down by 38.38% for h = 5 W/m^2 K, as ε rises to 0.85 from 0.05. This indicates that variation of surface coating of the cavity not only serves the same purpose as increasing the flow velocity but also probably gives the additional advantage of saving in pumping power requirement.

In order to understand the interactive effect of conduction and convection on T_{max}, Fig. 7 is drawn for a fixed input of q_v, ε and AR shown. Six typical values are considered for h encompassing the whole convection regime ($5 \leq h \leq 100$ W/m^2 K), while, for thermal conductivity, the lower and upper limits are taken to be 0.25 and 100 W/m K. The figure shows that k shows a greater influence on T_{max} in free convection dominant regime than in the regime of forced convection dominance. This is due to enhanced rate of heat conduction through the cavity with increasing k for smaller values of h, which gets diminished due to a comparatively much larger convective dissipation towards larger values of h. However, for a given k, holding other parameters fixed, there is a huge drop in T_{max} with increasing h. In the present example, for h = 5 W/m^2 K, T_{max} decreases by 39.44% between k = 0.25 W/m K and k = 100 W/m K. In contrast, for h = 100 W/m^2 K, a similar exercise as above brings down T_{max} just by 7.99%. Further, for k = 0.25 W/m K, T_{max} decreases by a very large 71.22% as h is raised from 5 to 100 W/m^2 K.

Interaction between internal conduction in the cavity and radiation from its surface in deciding the maximum temperature (T_{max}) attained by the cavity is shown in Fig. 8. Five

different values of ε and k considered for the present study and rest of the fixed input parameters are shown in the figure. A monotonic variation in T_{max}, for a given k, with ε is observed. An increasing rate of radiative dissipation from the rectangular cavity with ε brings down $T_{max,}$ for a given k. This observation again elucidates the role played by surface coating of the cavity in controlling T_{max} when other parameters are held fixed. In the example considered here, for k = 0.25 W/m K, replacing reflective coating with black paint, i.e., changing ε to 0.85 from 0.05, T_{max} could be brought down by as much as 39.02%. Further, it is also observed that holding ε fixed, one can bring down T_{max} by selecting a better conducting material for the rectangular cavity, which does the above job by shooting up the rate of conduction heat transfer. In the present example, calculations reveal that, for ε = 0.05, T_{max} comes down by 33.65% when a poor conductor (k = 0.25 W/m K) is replaced by a good conductor (k = 100 W/m K) with the other parameters held fixed.

Aspect ratio (AR) being one of the crucial parameters concerning the present problem, an attempt is made to study its role in peak temperature control. In this context, Fig. 9 shows T_{max} plotted against AR for three typical values of ε keeping q_v, k and h constant. It is clear that, for a given ε, T_{max} rises with AR. In particular, the above effect of AR on T_{max} is quite minimal for smaller ε, while it gets amplified towards larger values of ε. In the present example, for ε = 0.05, T_{max} rises only by 3.2% as AR is increased to 20 from 1. As against this, for ε = 0.85, a similar exercise shoots up T_{max} quite largely by 43.54%. This result indicates that it is not wise to use narrower cavities specifically when working with surface coatings with larger emissivity since it unduly increases the load on the cooling system.

Extending the study to further investigate the role of AR in the present problem, Fig.10 is drawn to exhibit the trend T_{max} follows with AR in different regimes of convection. Seven different values are opted for AR (1, 2, 4, 8, 12, 16 and 20) while four values of h are chosen, as shown. The figure also indicates the fixed input considered. As can be seen, T_{max} generally increases with AR in any given regime of convection. However, the above effect is quite feeble in forced convection dominant regime and reasonably perceivable in free convection dominant regime. In the present case, for h = 50 W/m^2 K, T_{max} is going up only by 1.27% as AR increases from 1 to 20. The same exercise, for h = 5 W/m^2 K, is bringing a 26.24% rise in T_{max}. It can be inferred from the present study that use of narrower cavities would lead to an inadvertent rise in

the peak temperature of the cavity and hence is discouraged particularly when working in free convection dominant regime.

The previous two studies threw light on the interaction of the geometric non-dimensional parameter AR with, respectively, ε and h, in influencing the peak cavity temperature. Another pertinent independent parameter that could influence T_{max} is the material property k. Thus, an attempt is made to look into coupling between AR and k in deciding the nature of variation of T_{max}, as shown in Fig. 11. The range for aspect ratios considered remain the same as that used earlier, while, for k, three values (0.25, 0.5 and 1 W/m K) are selected. The figure even shows the fixed values of rest of the parameters chosen. For a given k, one notices an increase in T_{max} with AR, which is to a larger degree for smaller values of k, while it peters down for larger values of k. This may be attributed to progressively increasing conduction activity in the cavity with increasing k that tends to counterbalance the undesirable effect of AR on T_{max}. In the present example, for k = 0.25 W/m K, T_{max} increases by 26.24% as AR is increased from 1 to 20. In contrary to the above, increased rate of conduction cuts down the rise in T_{max} to 16.69% between the same limits of AR, for k = 1 W/m K. This study, yet again, cautions against bringing down the width of the cavity for reasons like space occupied or miniaturization or both specifically while working with lower conducting materials.

4.4 Extraction of exclusive effect of radiation on maximum temperature

The exclusive effect of radiation on local temperature distribution along the cavity has already been singled out in Fig.5. Continuing on this, the explicit effect of radiation on T_{max} is plotted in Fig.12 keeping the operating conditions, viz., q_v, AR and k constant, as shown. Two distinct cases, one that ignores radiation and the other that considers maximum possible radiation, are simulated by considering ε = 0 and ε = 0.99, respectively. Six typical values are opted for h, from within the whole range of convection regime ($5 \leq h \leq 100$ W/m^2 K). The figure elucidates gross errors that could creep in the cooling load calculations upon ignoring radiation specifically while working in free convection dominant regime. As one moves towards forced convection dominant regime, though the above observation stands, the error that creeps in the calculation of T_{max} is quite negligible. In the present example, pertaining to the input shown in the figure, for h = 5 W/m^2 K, T_{max} comes down by 45.32% when once ε alone is increased from 0 to 0.99. A similar exercise made for h = 50 W/m^2 K brings down T_{max} just by 3.25%.

4.5 Roles played by convection and radiation in heat dissipation from the cavity

Any cooling system employed to abstract the heat generated by a given geometry does so through combined modes of convection and radiation as long as it uses a gaseous medium (like air). It is thus decided to explore the nature of variation of contributions of convection and radiation with surface emissivity (ε) for three representative values of h (5, 10 and 25 $W/m^2 K$). The values selected for ε and the rest of the parameters that are held constant are shown in Fig. 13 that narrates the results of the above study. It can be seen that, for a given h, the contribution of convection monotonically decreases with ε that is accompanied by a corresponding progressive increase in the contribution from radiation. Though the above observation is generally valid in any regime of convection (for any value of h), comparatively more perceivable results are noticed in buoyancy dominating flow (for smaller values of h). In the present example, for h = 5 $W/m^2 K$, altering the cavity surface from good reflector (say aluminum sheet) to good emitter (say black paint) brings down convection dissipation from 91.84% to 70.17% with a mirror image increase from 8.16% to 29.83% exhibited by radiative dissipation. By the same token, increasing h to 25 $W/m^2 K$ and bringing a similar transformation in the surface of the cavity, one notices a comparatively smaller drop in convective dissipation from 98.79% to 93.34% with its radiation counterpart undergoing an appropriate rise from 1.21% to 6.66%. The above may be attributed to the overriding effect of convection towards larger values of h, making heat dissipation relatively insensitive to surface coating.

The role aspect ratio (AR) plays, in conjunction with h (regime of convection), in deciding the contributory roles of convection and radiation in carrying the heat load in the cavity could be seen from Fig. 14. The entire range for AR ($1 \leq AR \leq 20$) is chosen with seven typical values of it opted for. The figure shows the values of h and the remaining input parameters pertaining to the study. The figure, in general, shows that, for a given h, the contribution to heat dissipation from convection increases with AR rather sharply to begin with before subsequently getting asymptotic. The above trend exhibited by convection is reflected in that of radiation, which drops sharply with AR initially and later undergoes a comparatively insignificant change. Though a similar variation is found for all the three values of h chosen, there is an obviously diminishing role from radiation towards forced convection regime due to the overriding influence of convection. In the present example, for h = 5 $W/m^2 K$, radiation contributes to

29.82% for AR = 1, while for the same value of AR, for h = 25 W/m^2 K, the contribution from radiation is very meagre and is 6.66%. It is to be noted that the above study pertains to $\varepsilon = 0.85$. If one were to use the best possible emitter (like lamp black with $\varepsilon = 0.99$) for the cavity, there would have been an increased inclination towards radiation cutting across the values of h chosen.

Figure 15 is plotted in order to understand as to how the geometric parameter AR, together with surface property ε, influences the relative contributory roles of convection and radiation. For ε, the same typical input between 0.05 and 0.85 as used in various other studies is employed. For AR, the lower limit is 0.25 implying a very wide cavity (W = 4L), while the upper limit is 16, which signifies a very narrow cavity (W = 0.0625L). The figure shows even the rest of the parameters that are held fixed. For a given AR, the contribution from convection decreases with ε rather sharply to begin with and relatively mildly thereafter. The above decrement in the role of convection is understandably manifested as a corresponding increase in the role of radiation. However, the above effect of ε on the contributions of convection and radiation peters down when once broader cavities are replaced with comparatively narrower cavities. It can be seen that, for AR = 16, there is hardly anything to choose between $\varepsilon = 0.05$ and $\varepsilon = 0.85$ with not much of a change noticed in the corresponding contributions. In the present example, for AR = 0.25, a change in ε from 0.05 to 0.85 helps in augmenting radiation contribution from 8.60% to 40.18%. In contrast to the above, for AR = 16, the radiation contribution is 2.08% for 0.05 and 3.25% for 0.85 thus substantiating the observation made already.

CONCLUDING REMARKS

Simulation studies on the effect of surface radiation on conjugate convection from a discretely heated rectangular cavity that is mounted with four non-identical and flush-mounted discrete heat sources have been taken up in the present paper. The effects of aspect ratio, surface emissivity, thermal conductivity and convection heat transfer coefficient have been exhaustively probed into. The transformation that one can bring in the thermal behaviour of the cavity through control of any single independent governing parameter even when the others could not be controlled has been lucidly brought out through various explicit studies performed. The gross errors that may creep in if one overlooks radiation have been quantitatively highlighted. A clear

delineation between convection and radiation is presented throwing light on their relative importance.

REFERENCES

1. Zinnes, A.E. (1970) The coupling of conduction with laminar natural convection from a vertical flat plate with arbitrary surface heating. ASME J Heat Transf 92:528-534
2. Lee, S., and Yovanovich, M.M (1989) conjugate heat transfer from a vertical plate with discrete heat sources under natural convection, ASME J Electronic Packaging, 111:261-267
3. Kang, B.H. and Jaluria, Y. (1990) Natural convection heat transfer characteristics of a protruding thermal source located on horizontal and vertical surfaces, Int J Heat Mass Transf, 33:1347 - 1357
4. Kishinami, K., Saito, H., Suzuki, J. (1995) Combined forced and free laminar convective heat transfer from a vertical plate with coupling of discontinuous surface heating. Int J Numer Methods Heat Fluid Flow 5:839-851
5. Cole, K. D. (1997) Conjugate heat transfer from a small heated strip. Int J Heat Mass Transf 40:2709-2719
6. Mendez, F. and Trevino, C. (2000) The conjugate conduction-natural convection heat transfer along a thin vertical plate with non-uniform internal heat generation. Int J Heat Mass Transf 43:2739-2748
7. Gururaja Rao, C., Balaji, C., Venkateshan, S.P. (2001) Conjugate mixed convection with surface radiation from a vertical plate with a discrete heat source. ASME J Heat Transf 123:698-702
8. Gururaja Rao, C. (2004) Buoyancy-aided mixed convection with conduction and surface radiation from a vertical electronic board with a traversable discrete heat source. Numerical Heat Transf A 45:935-956
9. Kanna, P.R. and Das, M.K. (2005) Conjugate forced convection heat transfer from a flat plate by laminar plane wall jet flow. Int J Heat Mass Tranf 48:2896-2910
10. Gururaja Rao, C., Venkata Krishna, A., Naga Srinivas, P. (2005) Simulation studies on multimode heat transfer from a square shaped electronic device with multiple discrete heat sources. Numer Heat Transf Part A 48:427-446

11. Gururaja Rao, C. (2007) Interaction of surface radiation with conduction and convection from a vertical channel with multiple discrete heat sources in the left wall. Numer Heat Transf Part A 52:831-848
12. Sawant, S.M. and Gururaja Rao, C. (2010) Combined conduction-mixed convection-surface radiation from a uniformly heated vertical plate. Int J Chem Eng Commun 197:881-899
13. Ganesh Kumar, G. and Gururaja Rao, C. (2012) Parametric studies and correlations for combined conduction-mixed convection-radiation from a non-identically and discretely heated vertical plate. Int J Heat Mass Tranf 48:505-517

FIGURE CAPTIONS

Figure 1 Schematic of the rectangular cavity considered along with system of coordinates

Figure 2 Local temperature distribution along **(a)** left, **(b)** bottom and **(c)** right walls of the cavity for different surface emissivities

Figure 3 Local temperature distribution along **(a)** left, **(b)** bottom and **(c)** right walls of the cavity in various regimes of convection

Figure 4 Local temperature distribution along **(a)** left, **(b)** bottom and **(c)** right walls of the cavity for different thermal conductivities

Figure 5 Local temperature along **(a)** left and **(b)** right walls of the cavity without and with radiation taken into reckoning

Figure 6 Variation of peak temperature of the cavity with surface emissivity in various regimes of convection

Figure 7 Variation of peak temperature of the cavity with convection heat transfer coefficient for different thermal conductivities

Figure 8 Variation of peak temperature with surface emissivity for different thermal conductivities of the cavity

Figure 9 Variation of maximum temperature of the cavity with aspect ratio for different surface emissivities

Figure 10 Variation of maximum temperature of the cavity with aspect ratio in different regimes of convection

Figure 11 Variation of maximum temperature of the cavity with aspect ratio for different thermal conductivities

Figure 12 Extraction of exclusive effect of radiation on maximum temperature of the cavity in different convection regimes

Figure 13 Relative contributions of convection and radiation with surface emissivity in different regimes of convection

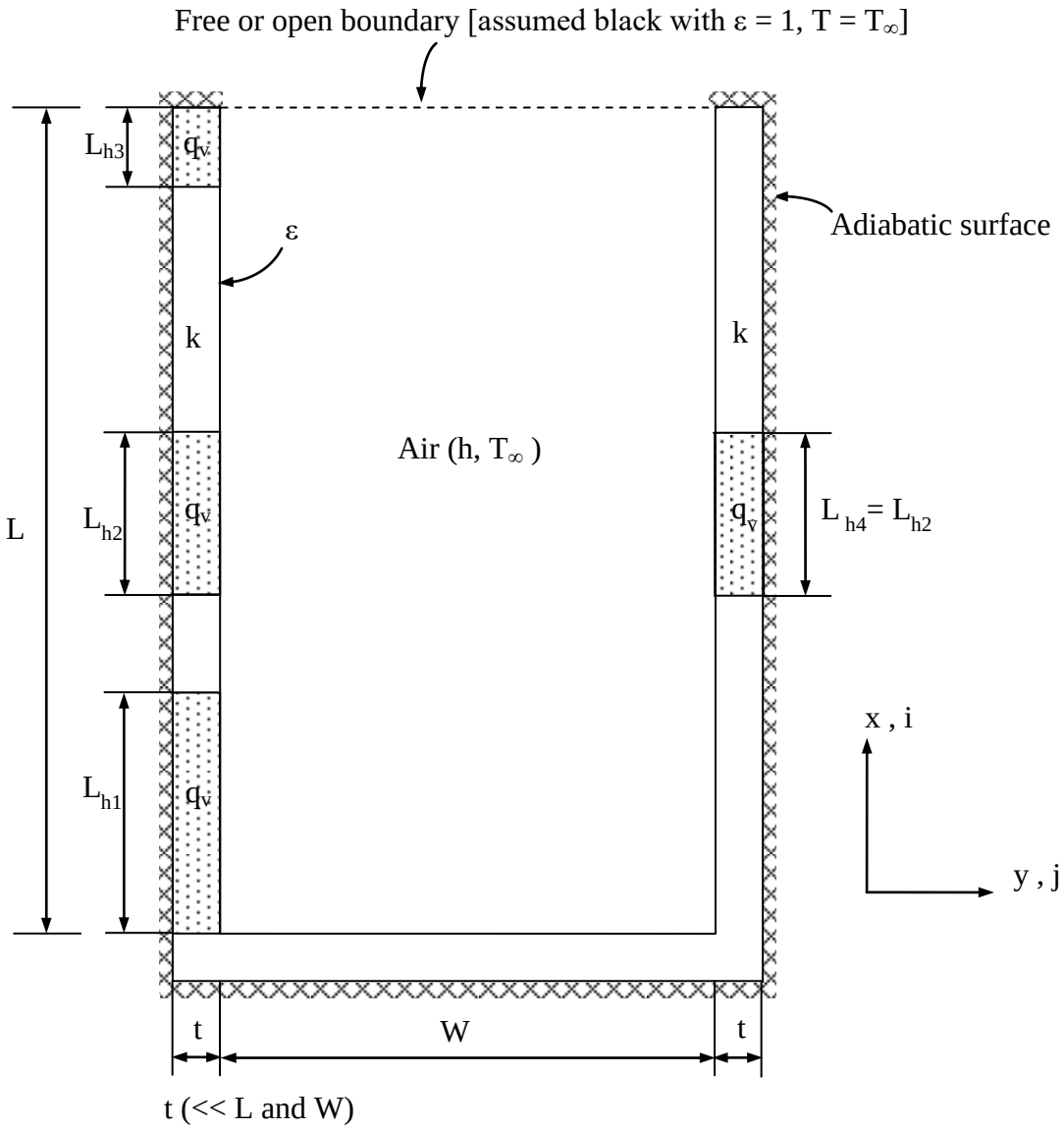
Free or open boundary [assumed black with ε = 1, T = T∞]
Lh3
qv
ε
Adiabatic surface
k
k
Air (h, T∞)
L
Lh2
qv
qv
L h4= Lh2
x , i
Lh1
qv
y , j
t
W
t
t (<< L and W)

Fig. 1

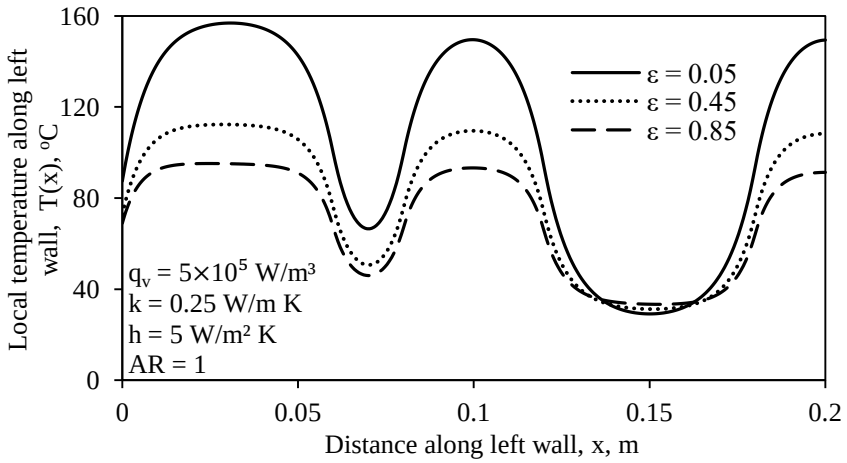
Local temperature along left wall, T(x), ºC
Distance along left wall, x, m
ε = 0.05
ε = 0.45
ε = 0.85
$q_v = 5\times10^5$ W/m³
k = 0.25 W/m K
h = 5 W/m² K
AR = 1
0
40
80
120
160
0
0.05
0.1
0.15
0.2

(a)

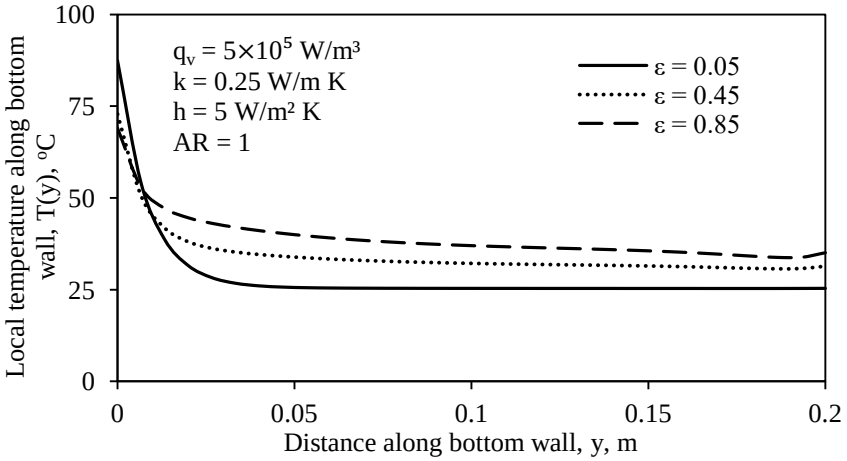
Local temperature along bottom wall, T(y), ºC
Distance along bottom wall, y, m
ε = 0.05
ε = 0.45
ε = 0.85
$q_v = 5\times10^5$ W/m³
k = 0.25 W/m K
h = 5 W/m² K
AR = 1
0
25
50
75
100
0
0.05
0.1
0.15
0.2

(b)

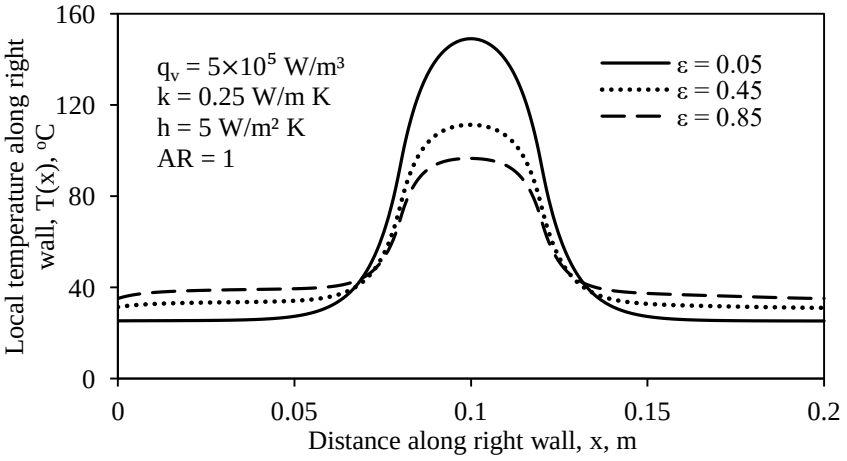
Local temperature along right wall, T(x), ºC
Distance along right wall, x, m
ε = 0.05
ε = 0.45
ε = 0.85
$q_v = 5\times10^5$ W/m³
k = 0.25 W/m K
h = 5 W/m² K
AR = 1
0
40
80
120
160
0
0.05
0.1
0.15
0.2

(c)

Fig. 2

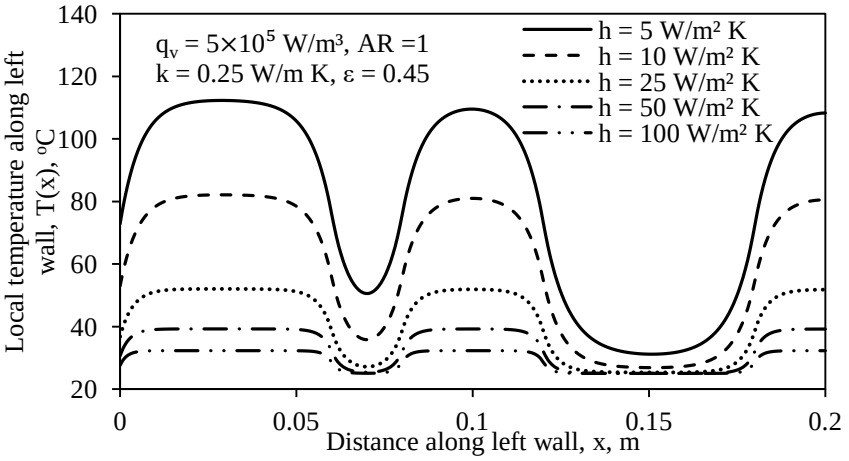
$q_v = 5\times10^5$ W/m³, AR =1
k = 0.25 W/m K, ε = 0.45
h = 5 W/m² K
h = 10 W/m² K
h = 25 W/m² K
h = 50 W/m² K
h = 100 W/m² K
Local temperature along left wall, T(x), ºC
Distance along left wall, x, m

(a)

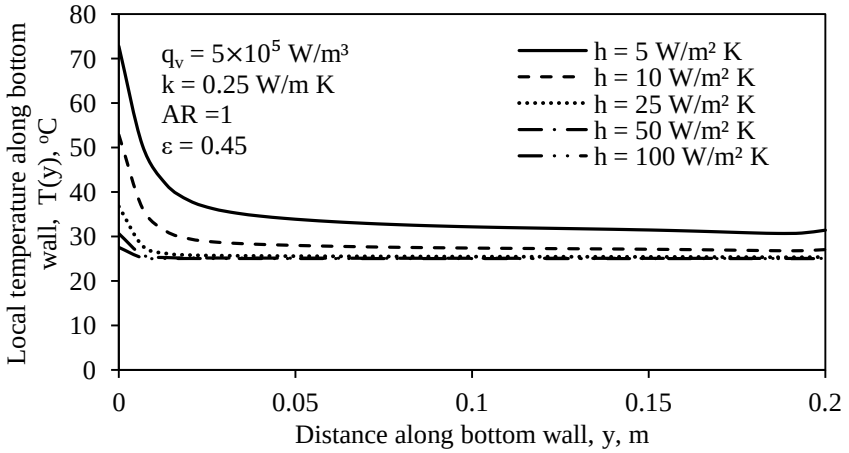
$q_v = 5\times10^5$ W/m³
k = 0.25 W/m K
AR =1
ε = 0.45
h = 5 W/m² K
h = 10 W/m² K
h = 25 W/m² K
h = 50 W/m² K
h = 100 W/m² K
Local temperature along bottom wall, T(y), ºC
Distance along bottom wall, y, m

(b)

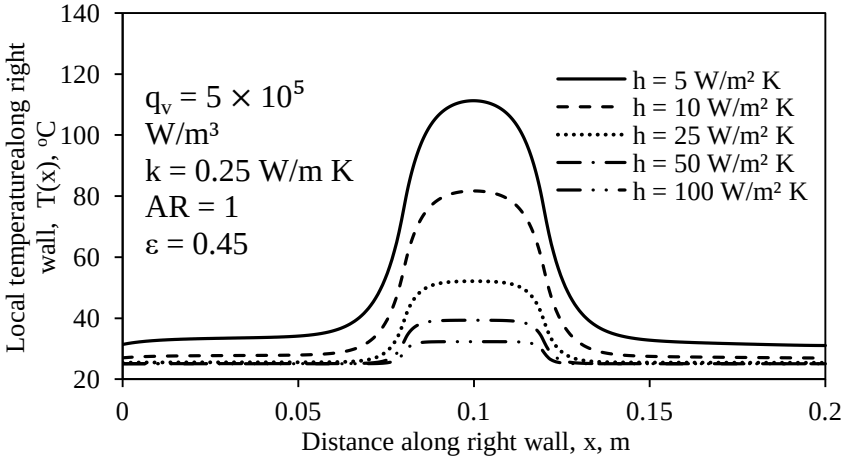
$q_v = 5 \times 10^5$ W/m³
k = 0.25 W/m K
AR = 1
ε = 0.45
h = 5 W/m² K
h = 10 W/m² K
h = 25 W/m² K
h = 50 W/m² K
h = 100 W/m² K
Local temperaturealong right wall, T(x), ºC
Distance along right wall, x, m

(c)

Fig. 3

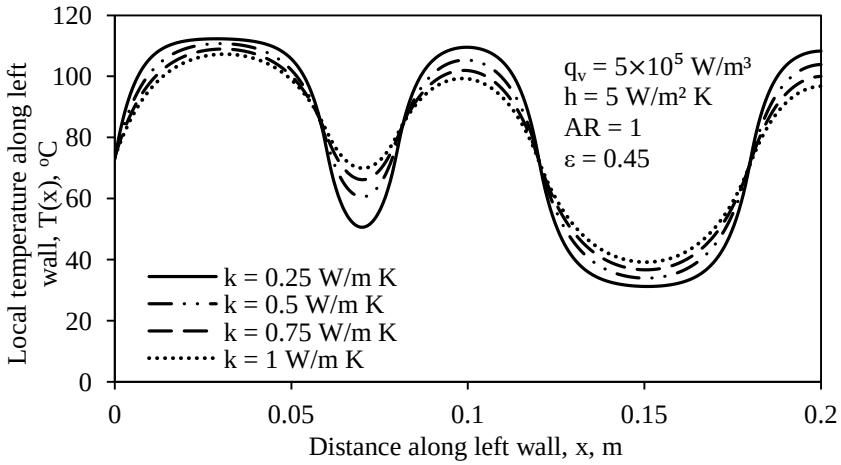
Local temperature along left wall, T(x), °C
Distance along left wall, x, m
$q_v = 5\times10^5$ W/m³
h = 5 W/m² K
AR = 1
ε = 0.45
k = 0.25 W/m K
k = 0.5 W/m K
k = 0.75 W/m K
k = 1 W/m K

(a)

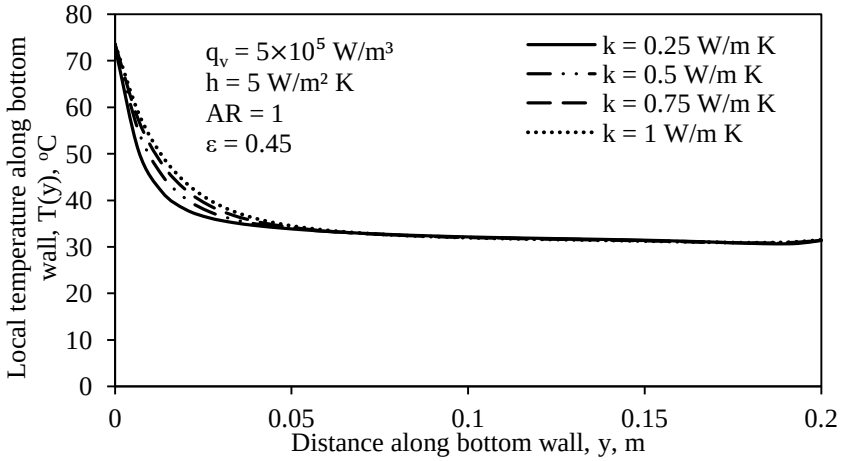
Local temperature along bottom wall, T(y), °C
Distance along bottom wall, y, m
$q_v = 5\times10^5$ W/m³
h = 5 W/m² K
AR = 1
ε = 0.45
k = 0.25 W/m K
k = 0.5 W/m K
k = 0.75 W/m K
k = 1 W/m K

(b)

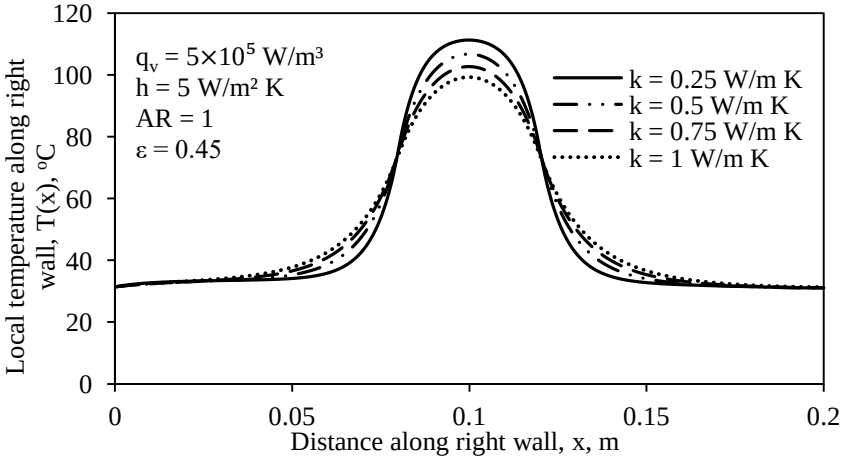
Local temperature along right wall, T(x), °C
Distance along right wall, x, m
$q_v = 5\times10^5$ W/m³
h = 5 W/m² K
AR = 1
ε = 0.45
k = 0.25 W/m K
k = 0.5 W/m K
k = 0.75 W/m K
k = 1 W/m K

(c)

Fig. 4

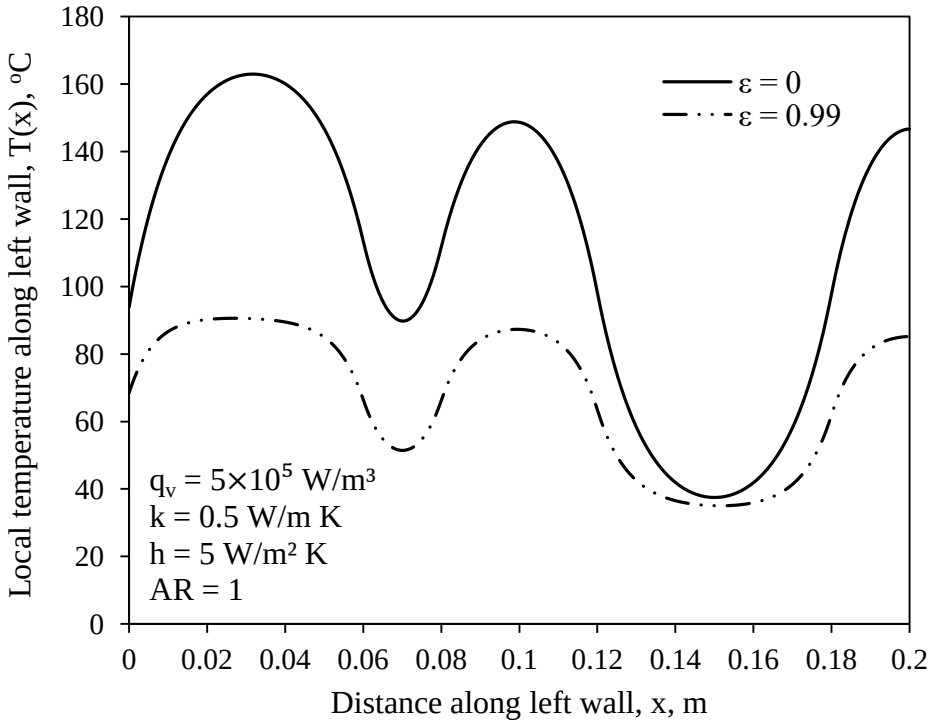
Local temperature along left wall, T(x), °C
Distance along left wall, x, m
ε = 0
ε = 0.99
$q_v = 5\times10^5$ W/m³
k = 0.5 W/m K
h = 5 W/m² K
AR = 1

(a)

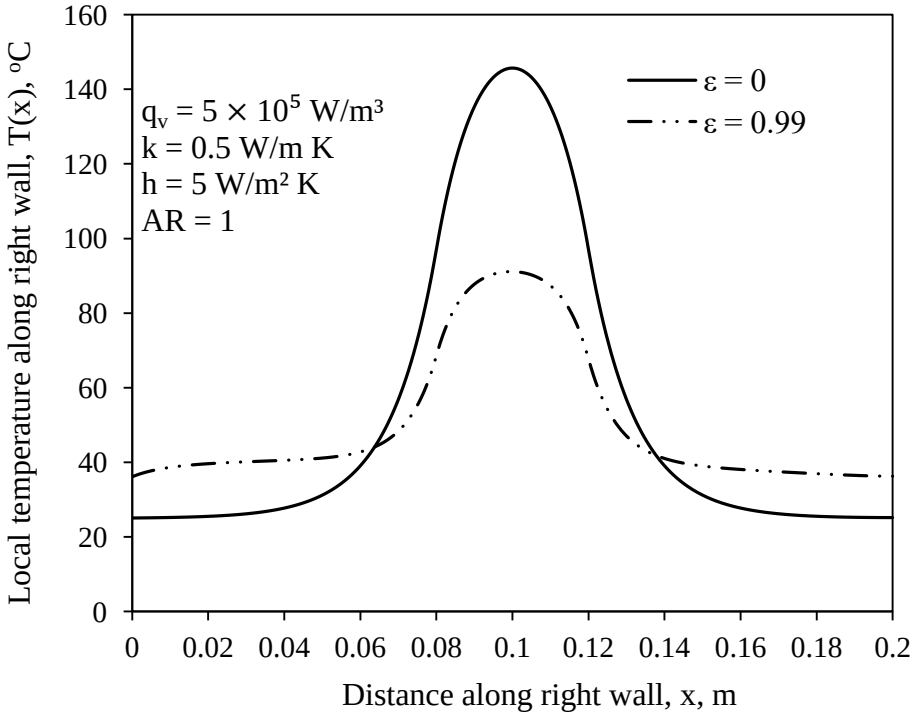
Local temperature along right wall, T(x), °C
Distance along right wall, x, m
ε = 0
ε = 0.99
$q_v = 5 \times 10^5$ W/m³
k = 0.5 W/m K
h = 5 W/m² K
AR = 1

(b)

Fig. 5

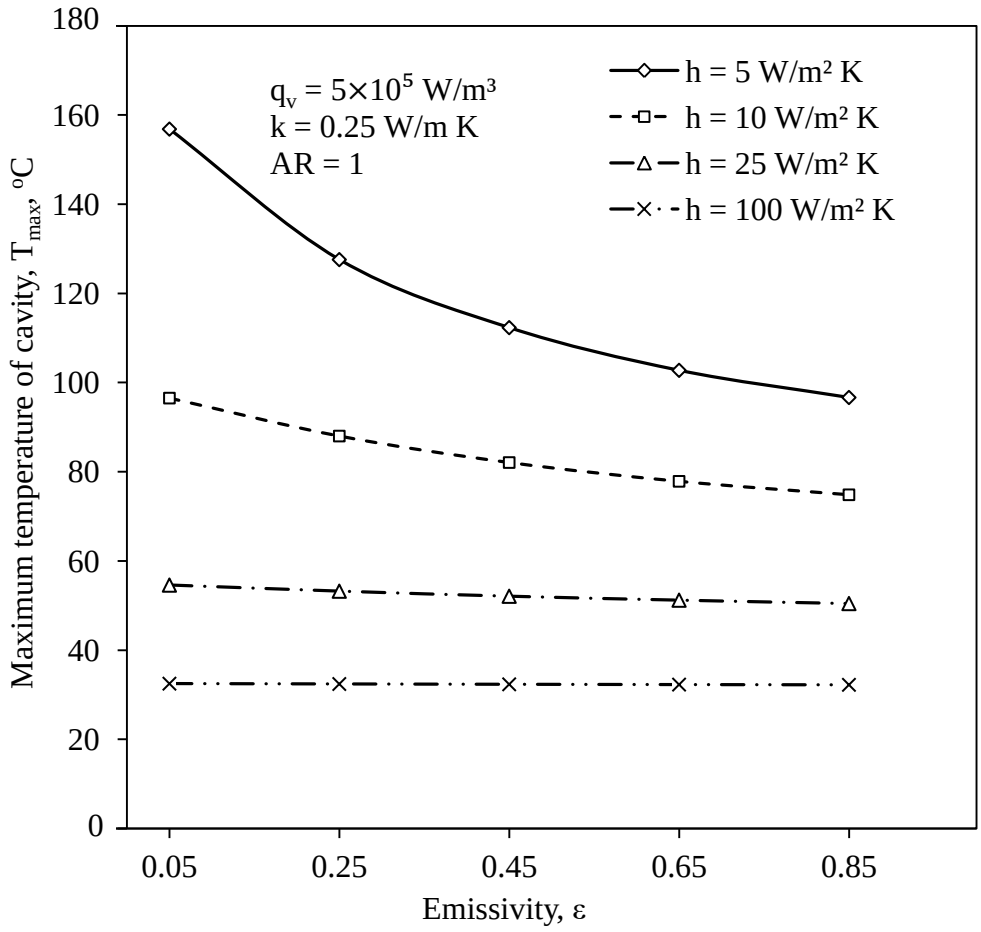
180
160
140
120
100
80
60
40
20
0
0.05
0.25
0.45
0.65
0.85
Emissivity, ε
Maximum temperature of cavity, T_{max}, °C
$q_v = 5\times10^5$ W/m³
k = 0.25 W/m K
AR = 1
h = 5 W/m² K
h = 10 W/m² K
h = 25 W/m² K
h = 100 W/m² K

Fig. 6

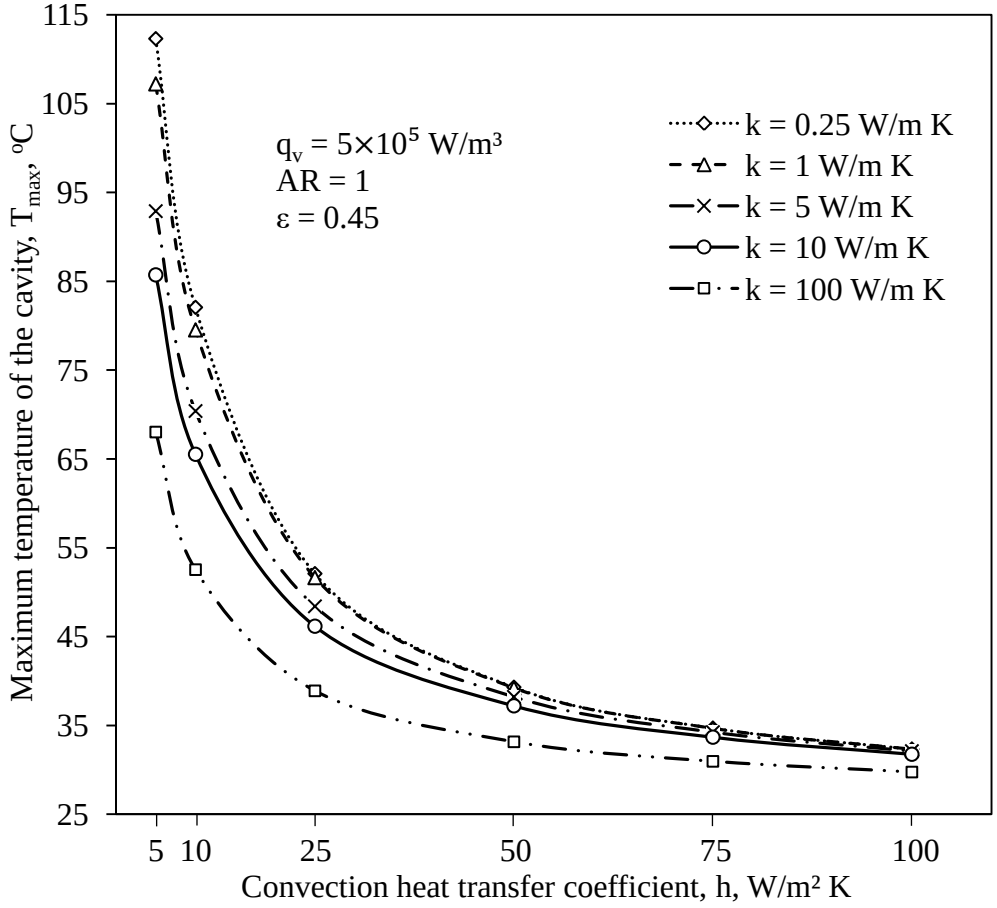
115
105
95
85
75
65
55
45
35
25
Maximum temperature of the cavity, T_{max}, °C
$q_v = 5\times10^5$ W/m³
AR = 1
ε = 0.45
k = 0.25 W/m K
k = 1 W/m K
k = 5 W/m K
k = 10 W/m K
k = 100 W/m K
5
10
25
50
75
100
Convection heat transfer coefficient, h, W/m² K

Fig. 7

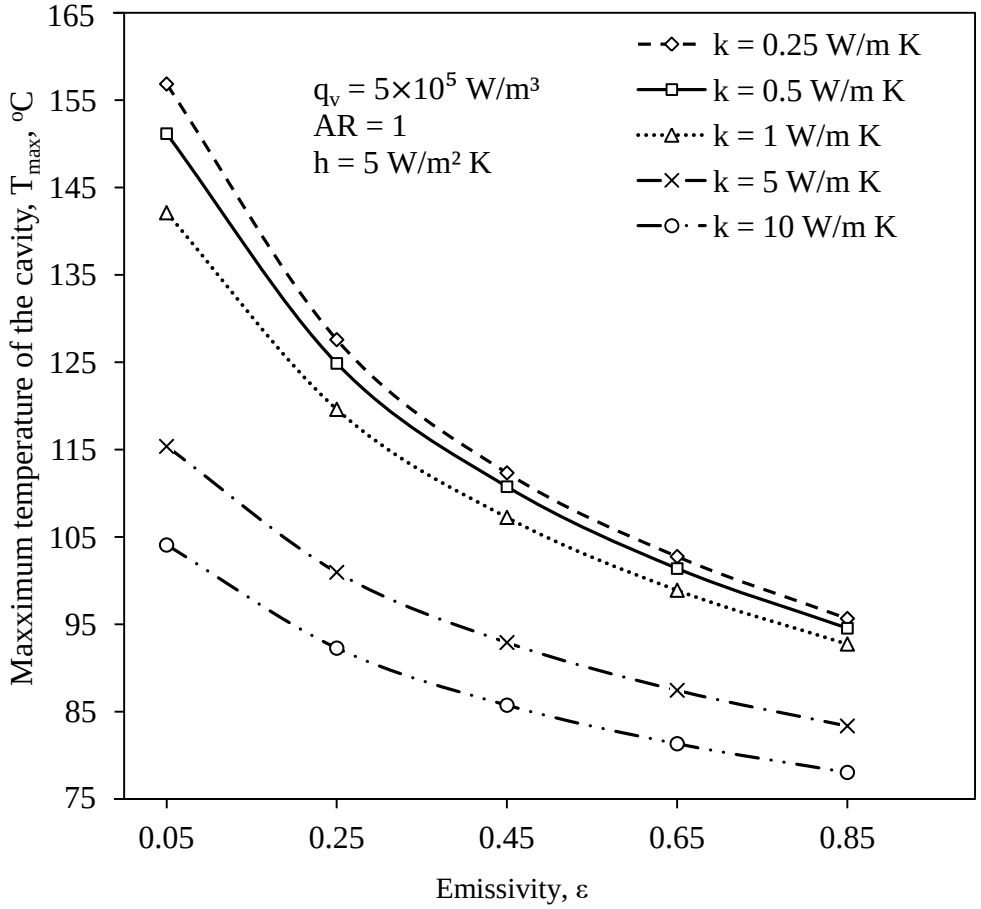
165
155
145
135
125
115
105
95
85
75
0.05
0.25
0.45
0.65
0.85
Maxximum temperature of the cavity, T_{max}, ºC
Emissivity, ε
$q_v = 5\times10^5$ W/m³
AR = 1
h = 5 W/m² K
k = 0.25 W/m K
k = 0.5 W/m K
k = 1 W/m K
k = 5 W/m K
k = 10 W/m K

Fig. 8

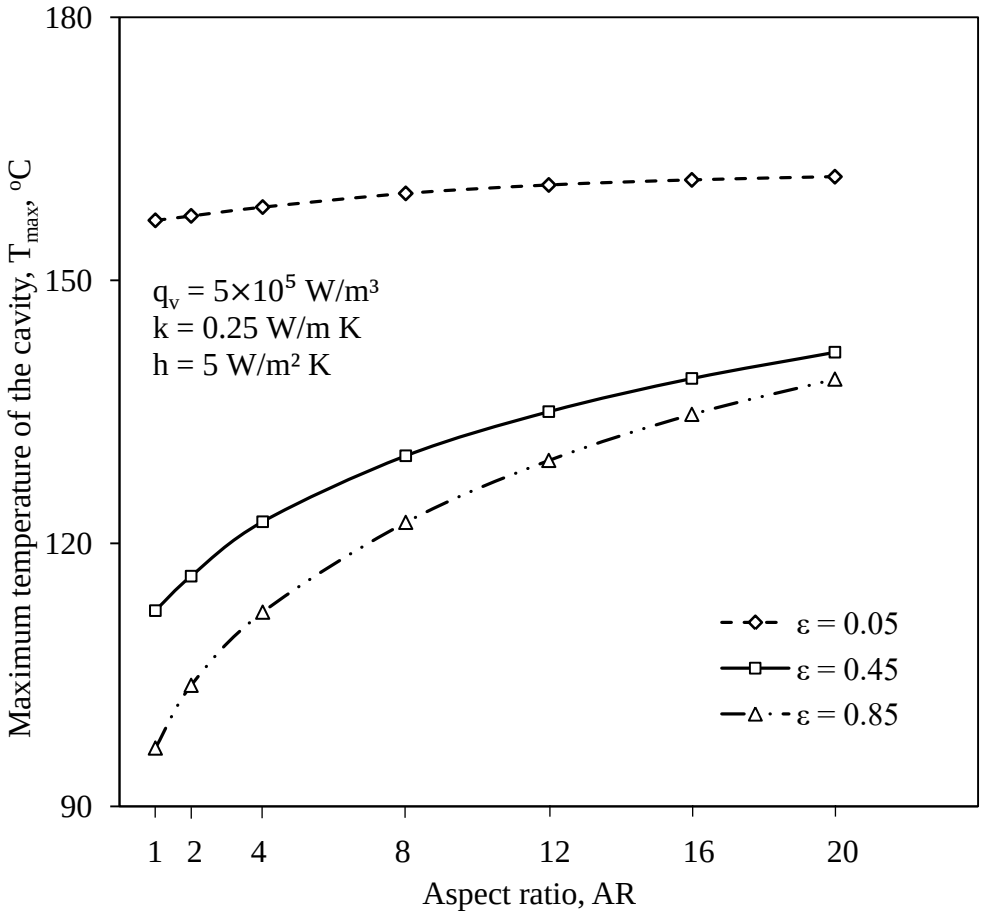
180
150
120
90
Maximum temperature of the cavity, T_{max}, °C
$q_v = 5\times10^5$ W/m³
k = 0.25 W/m K
h = 5 W/m² K
ε = 0.05
ε = 0.45
ε = 0.85
1
2
4
8
12
16
20
Aspect ratio, AR

Fig. 9

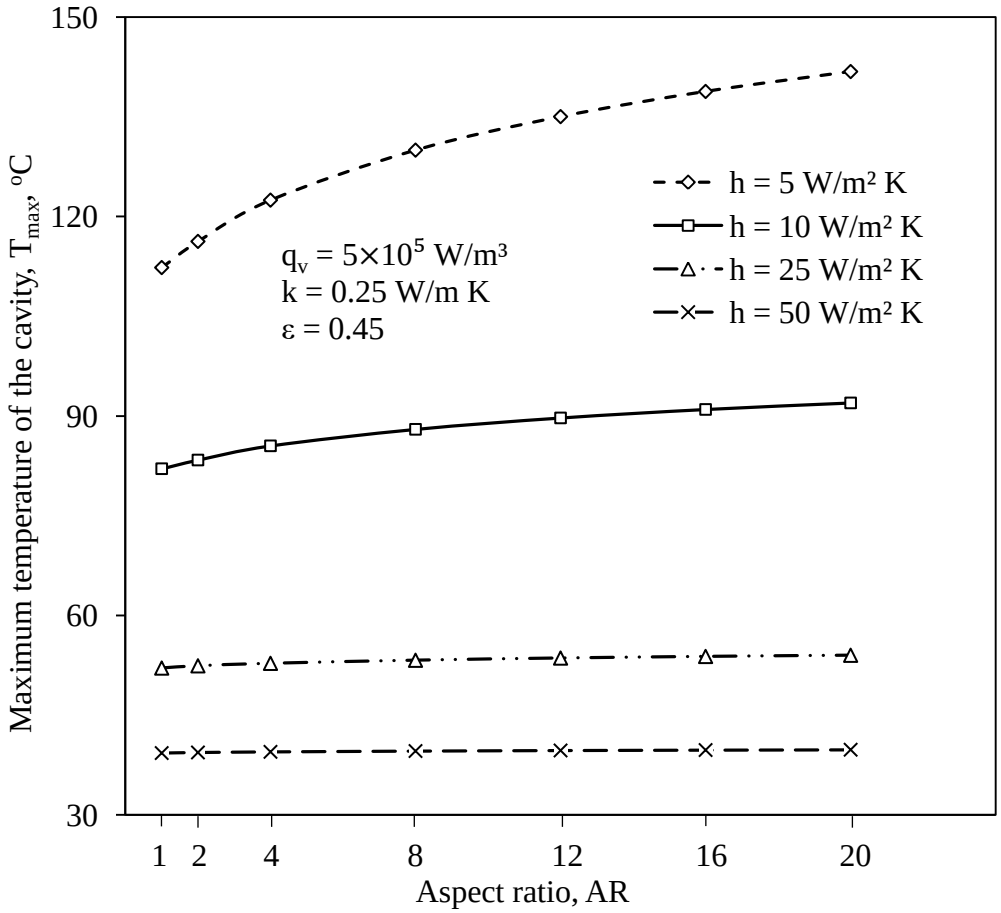
150
120
90
60
30
Maximum temperature of the cavity, T_{max}, °C
$q_v = 5\times10^5$ W/m³
k = 0.25 W/m K
ε = 0.45
h = 5 W/m² K
h = 10 W/m² K
h = 25 W/m² K
h = 50 W/m² K
1
2
4
8
12
16
20
Aspect ratio, AR

Fig. 10

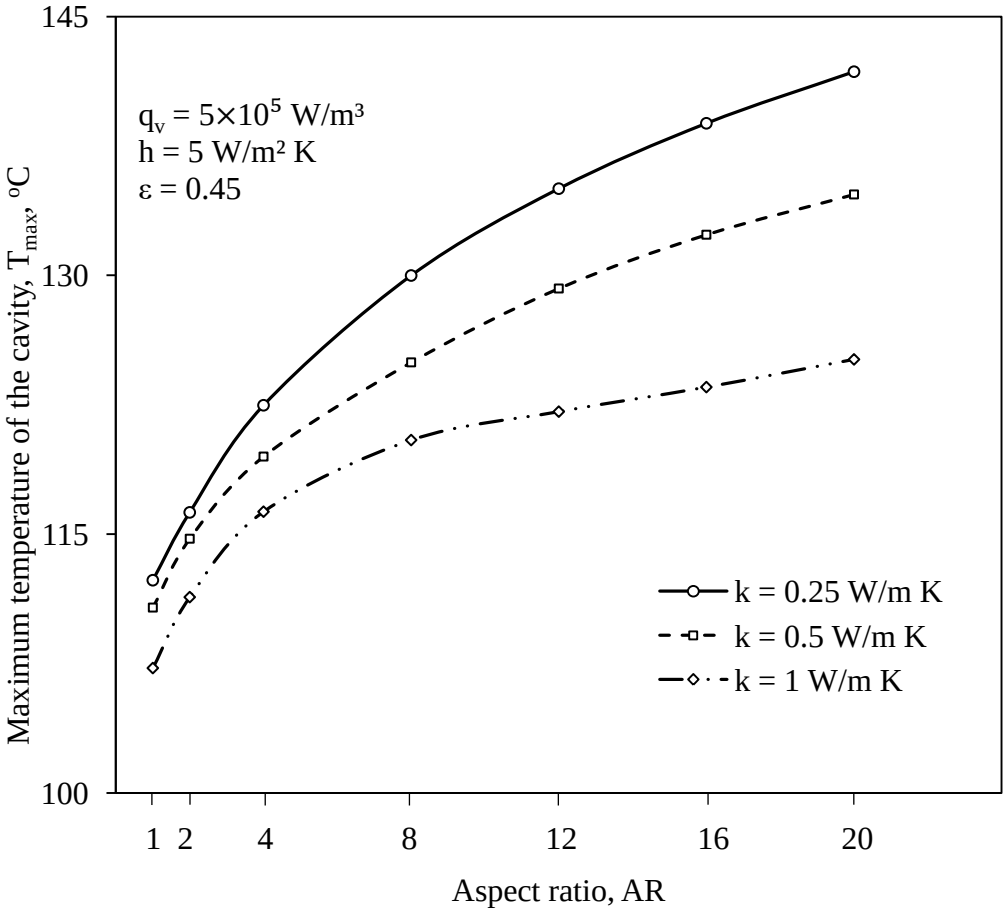
145
130
115
100
$q_v = 5\times10^5$ W/m³
h = 5 W/m² K
ε = 0.45
Maximum temperature of the cavity, T_{max}, °C
k = 0.25 W/m K
k = 0.5 W/m K
k = 1 W/m K
1
2
4
8
12
16
20
Aspect ratio, AR

Fig. 11

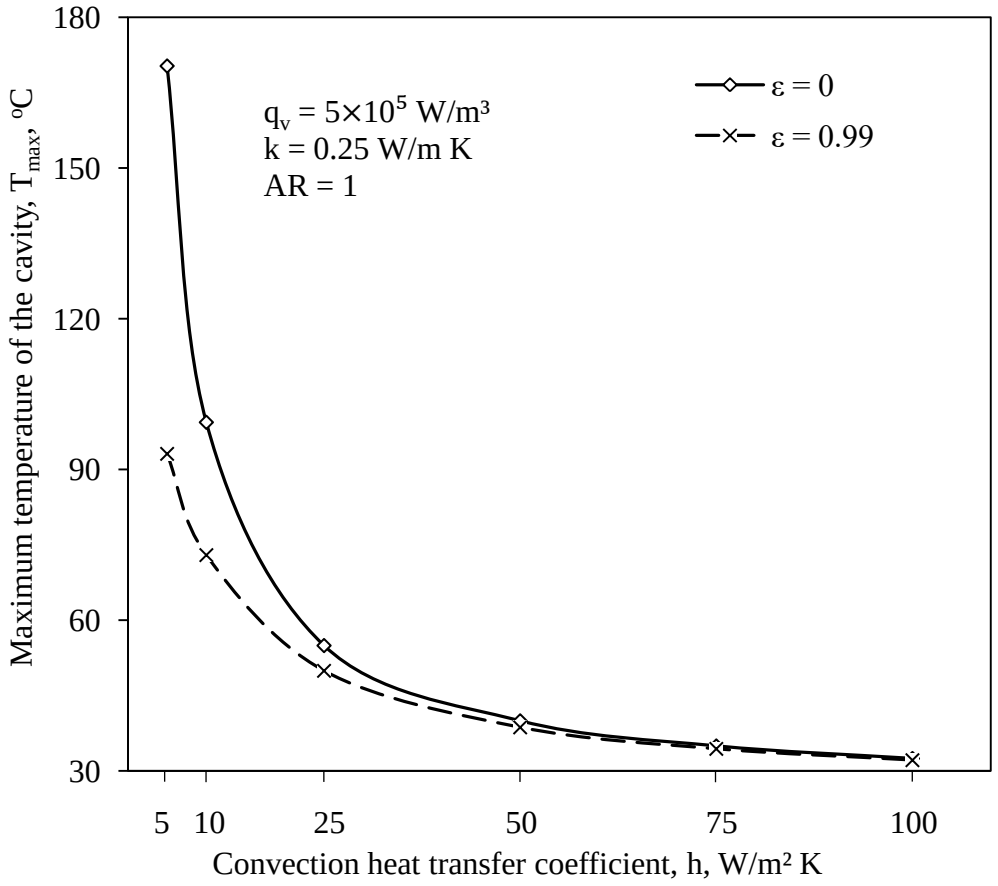
180
150
120
90
60
30
Maximum temperature of the cavity, T_{max}, °C
$q_v = 5\times10^5$ W/m³
k = 0.25 W/m K
AR = 1
ε = 0
ε = 0.99
5
10
25
50
75
100
Convection heat transfer coefficient, h, W/m² K

Fig. 12

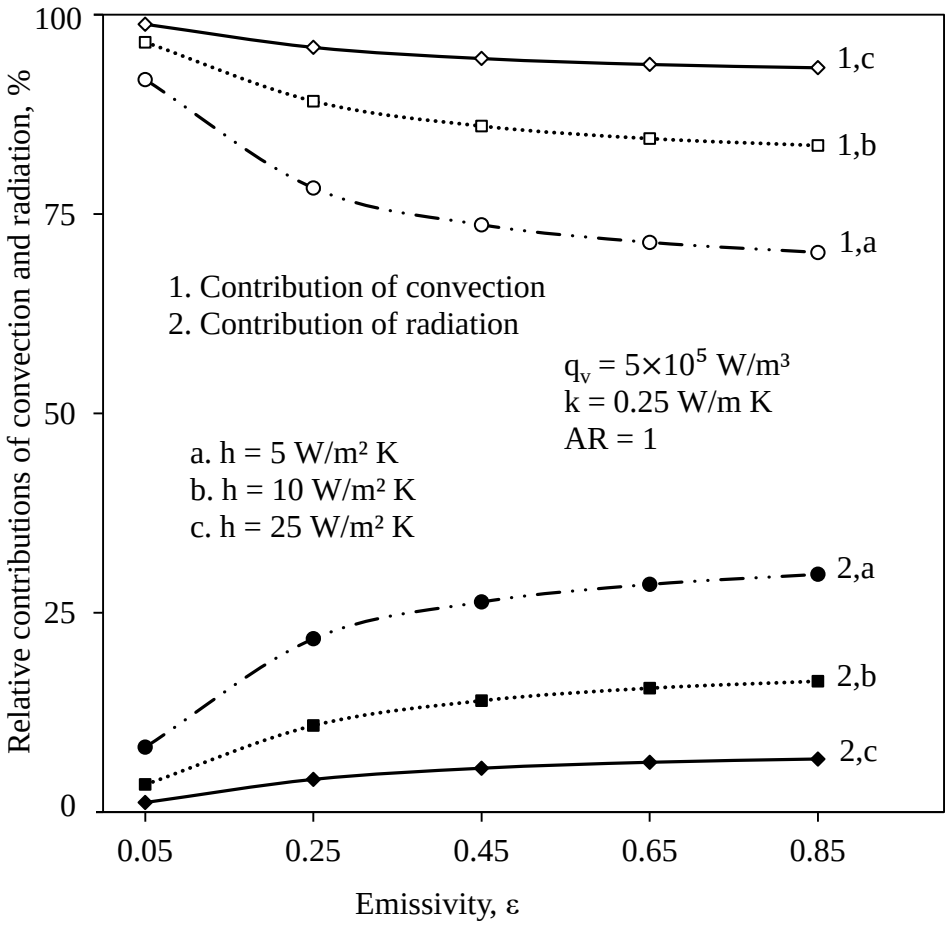
100
75
50
25
0
0.05
0.25
0.45
0.65
0.85
Relative contributions of convection and radiation, %
Emissivity, ε
1,c
1,b
1,a
1. Contribution of convection
2. Contribution of radiation
$q_v = 5\times10^5$ W/m³
k = 0.25 W/m K
AR = 1
a. h = 5 W/m² K
b. h = 10 W/m² K
c. h = 25 W/m² K
2,a
2,b
2,c

Fig. 13

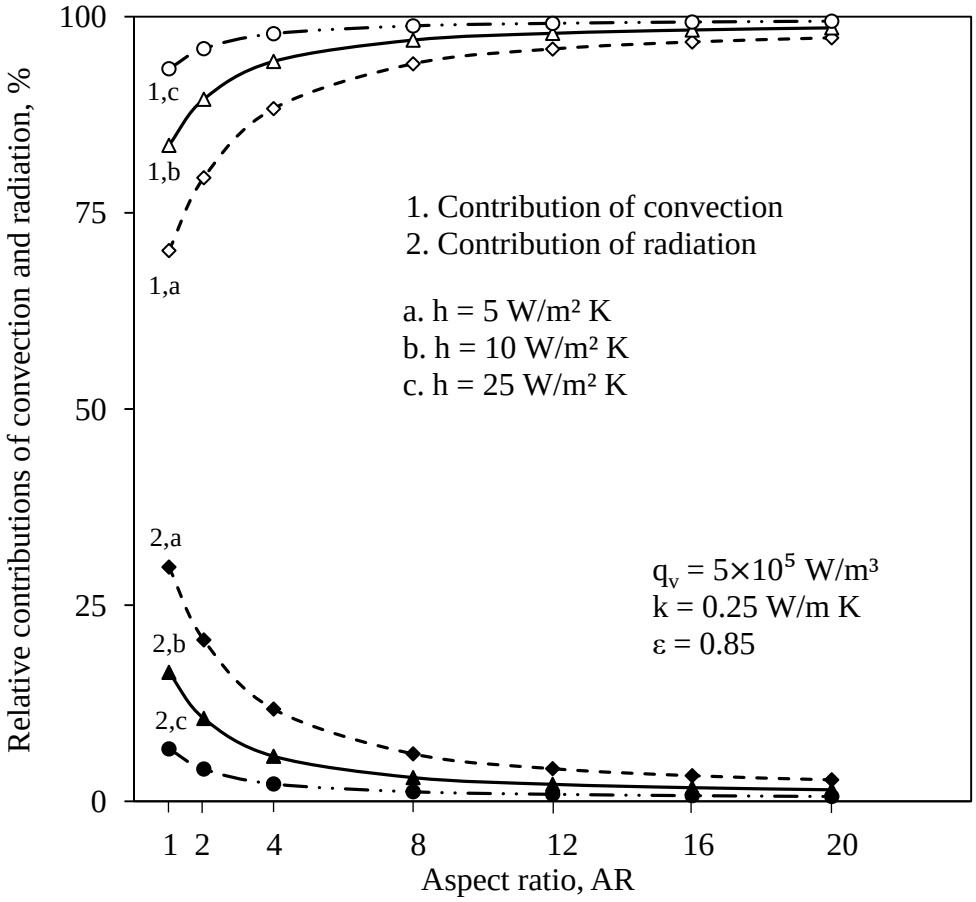
Relative contributions of convection and radiation, %
100
75
50
25
0
1,c
1,b
1,a
1. Contribution of convection
2. Contribution of radiation
a. h = 5 W/m² K
b. h = 10 W/m² K
c. h = 25 W/m² K
2,a
2,b
2,c
$q_v = 5\times10^5$ W/m³
k = 0.25 W/m K
ε = 0.85
1 2 4 8 12 16 20
Aspect ratio, AR

Fig. 14

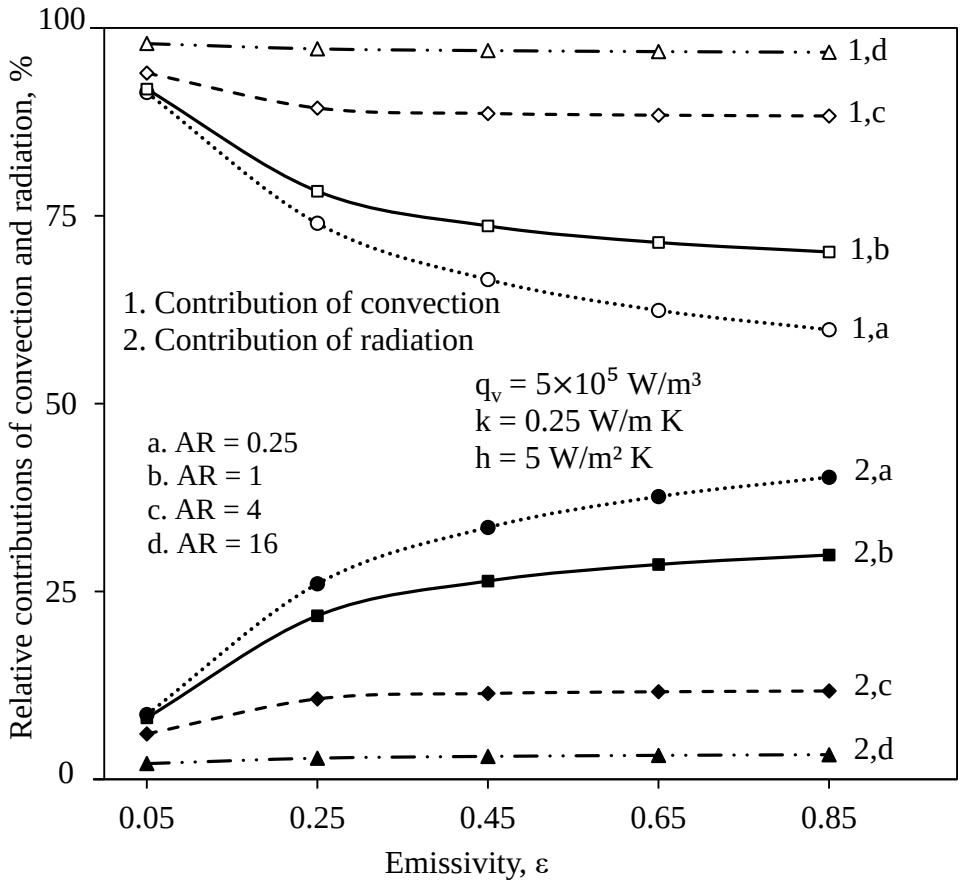
100
75
50
25
0
Relative contributions of convection and radiation, %
0.05
0.25
0.45
0.65
0.85
Emissivity, ε
1,d
1,c
1,b
1,a
1. Contribution of convection
2. Contribution of radiation
$q_v = 5\times10^5$ W/m³
k = 0.25 W/m K
h = 5 W/m² K
a. AR = 0.25
b. AR = 1
c. AR = 4
d. AR = 16
2,a
2,b
2,c
2,d

Fig. 15